Measurement of high-Q^2 deep inelastic scattering cross sections with longitudinally polarised positron beams at HERA

Julian Rautenberg
On behalf of the H1 and ZEUS collaborations
Physikalisches Institut, Universität Bonn, Nussallee 12, 53115 Bonn, Germany
supported by the German Federal Ministry for Education and Research (BMBF)

The first measurements of the cross sections for neutral and charged current deep inelastic scattering in e^+p collisions with longitudinally polarised positron beams are presented. The total cross section for e^+p charged current deep inelastic scattering is presented at positive and negative values of positron beam longitudinal polarisation for an integrated luminosity of $37.0\,\mathrm{pb}^{-1}$ H1 data and $30.5\,\mathrm{pb}^{-1}$ ZEUS data collected in 2003 and 2004 at a centre-of-mass energy of 319 GeV. In addition, the ZEUS collaboration measured the single differential cross sections for charged and neutral current deep inelastic scattering in the kinematic region $Q^2 > 200\,\mathrm{GeV}^2$. The measured cross sections are compared with the predictions of the Standard Model. The H1 collaboration extrapolate the cross section to a fully left handed positron beam and find it to be consistent with the Standard Model expectation.

1 Introduction

Deep inelastic scattering (DIS) of leptons off nucleons has proved to be a key tool in the understanding of the structure of the proton and the form of the Standard Model (SM). The HERA *ep* collider has made possible the exploration of DIS at high values of negative four-momentum-transfer squared, Q^2. Using data taken in the years 1994-2000 the H1 and ZEUS collaborations have reported measurements of the cross sections for charged current (CC) and neutral current (NC) DIS [1,2]. These measurements extend the kinematic region covered by fixed-target experiments [3] to higher Q^2 and allow the HERA experiments to probe the electroweak sector of the SM.

This paper presents the measurements of the cross sections for e^+p CC and NC DIS with longitudinally polarised positron beams. The measurements are based on the integrated luminosities collected at the luminosity weighted mean polarisations given in Table 1 with the ZEUS

	$\mathcal{L}/\,\mathrm{pb}^{-1}$	P
H1	15.3	+33.0%
	21.7	-40.2%
ZEUS	14.1	+31.8%
	16.4	-40.2%

Table 1: Integrated luminosities and the luminosity weighted mean longlitudinal polarisation of the lepton beam for the H1 and ZEUS data samples.

and H1 detectors in 2003 and 2004. During this time HERA collided protons of energy 920 GeV with positrons of energy 27.6 GeV, yielding collisions at a centre-of-mass energy of 319 GeV. The measured cross sections are compared to the SM predictions.

2 Polarised lepton beams

At HERA transverse polarisation of the lepton beam arises through synchrotron radiation via the Sokolov-Ternov effect [4]. As a part of the HERA upgrade in the year 2000 spin rotators that rotate the polarisation into the longitudinal direction were installed in the lepton beamline round the collision regions where the H1 and ZEUS detectors are located. The polarisation is continuously measured using two independent polarimeters. The TPOL[5] is situated at a position of transverse lepton beam polarisation, and the LPOL[6] at one of longitudinal polarisation. The luminosity weighted polarisation distribution for the data of the presented H1 measurement is shown in Fig. 1.

3 Kinematic variables and cross sections

Inclusive deep inelastic lepton-proton scattering can be described in terms of the kinematic variables x, y and Q^2. The variable Q^2 is defined to be $Q^2 = -q^2 = -(k-k')^2$ where k and k' are the four-momenta of the incoming and scattered lepton, respectively. Bjorken x is defined by $x = Q^2/2P\cdot q$ where P is the four-momentum of the incoming proton. The variable y is defined by $Q^2 = sxy$, where $s = 4E_eE_p$ is the square of the lepton-proton centre-of-mass energy (neglecting the masses of the incoming particles).

The electroweak Born level cross section for the CC reaction, $e^+p \rightarrow \bar{\nu}_e X$, with a longitudinally polarised positron beam (defined in Eqn. (2)), can be expressed as [7]

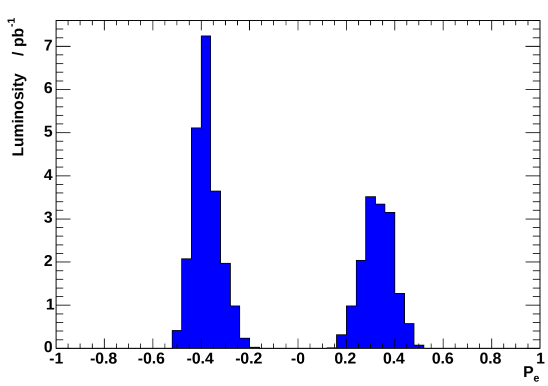

Figure 1: Distribution of luminosity versus the polarisation of the lepton beam, P_e, for the H1 data sample.

$$\frac{d^2\sigma^{CC}(e^+p)}{dxdQ^2} = (1+\mathcal{P})\frac{G_F^2}{4\pi x}\left(\frac{M_W^2}{M_W^2+Q^2}\right)^2 \cdot \left[Y_+F_2^{CC}(x,Q^2) - Y_-xF_3^{CC}(x,Q^2) - y^2F_L^{CC}(x,Q^2)\right], \tag{1}$$

where G_F is the Fermi constant, M_W is the mass of the W boson and $Y_\pm = 1 \pm (1-y)^2$. The structure functions F_2^{CC} and xF_3^{CC} contain sums and differences of the quark and anti-quark parton density functions (PDFs) and F_L^{CC} is the longitudinal structure function. The longitudinal polarisation of the positron beam is defined as

$$\mathcal{P} = \frac{N_R - N_L}{N_R + N_L}, \tag{2}$$

where N_R and N_L are the numbers of right and left-handed positrons in the beam. Similarly the cross section for the NC reaction, $e^+p \to e^+X$, can be expressed as

$$\frac{d^2\sigma^{NC}(e^+p)}{dxdQ^2} = \frac{2\pi\alpha^2}{xQ^4}[H_0^+ + \mathcal{P}H_{\mathcal{P}}^+], \tag{3}$$

where α is the QED coupling constant and H_0^+ and $H_{\mathcal{P}}^+$ contain the unpolarised and polarised structure functions, respectively.

Charged current events are characterised by a large missing transverse momentum, $P_{T,\mathrm{miss}}$, which is calculated by ZEUS as

$$P_{T,\mathrm{miss}}^2 = P_x^2 + P_y^2 = \left(\sum_i E_i \sin\theta_i \cos\phi_i\right)^2 + \left(\sum_i E_i \sin\theta_i \sin\phi_i\right)^2, \tag{4}$$

where the sum runs over all calorimeter energy deposits E_i, and θ_i and ϕ_i are the polar and azimuthal angles of the calorimeter cell as viewed from the interaction vertex. The hadronic polar angle, γ_h, is defined by $\cos\gamma_h = (P_{T,\mathrm{miss}}^2 - \delta^2)/(P_{T,\mathrm{miss}}^2 + \delta^2)$, where $\delta = \sum(E_i - E_i\cos\theta_i) = \sum(E - P_z)_i$. H1 uses an analog definition summing over all final state particles. In the naive Quark Parton Model, γ_h gives the scattering angle of the struck quark in the laboratory frame. The total transverse energy, E_T, is given by $E_T = \sum E_i \sin\theta_i$.

Neutral current events are characterised by the presence of a high-energy isolated scattered positron in the detector. It follows from longitudinal momentum conservation that for well measured NC events δ peaks at twice the positron beam energy i.e. 55 GeV.

The kinematic variables for charged current events were reconstructed from the measured $P_{T,\mathrm{miss}}$ and δ using the Jacquet-Blondel method [8]. For the neutral current events the ZEUS measurement uses the double-angle method [9] to estimate the kinematic variables from the polar angles of the scattered positron θ_e and the hadronic final state γ_h while H1 uses the $e\Sigma$ method [10] to estimate the kinematic quantities from the scattered positrons energy, its angle and δ.

4 Monte Carlo simulation

Monte Carlo simulation (MC) was used to determine the efficiency for selecting events, the accuracy of kinematic reconstruction, to estimate the background rate and to deduce cross sections for the full kinematic region from the data. A sufficient number of events were generated to ensure that uncertainties from MC statistics were small. The MC samples were normalised to the total integrated luminosity of the data.

Neutral and charged current DIS events including radiative effects were simulated using the DJANGOH [11] generator. The hadronic final state was simulated using the colour-dipole model of ARIADNE [12]. For the hadronisation the Lund string model of JETSET 7.4 [13] is used. Additional samples used are as described in [1,2].

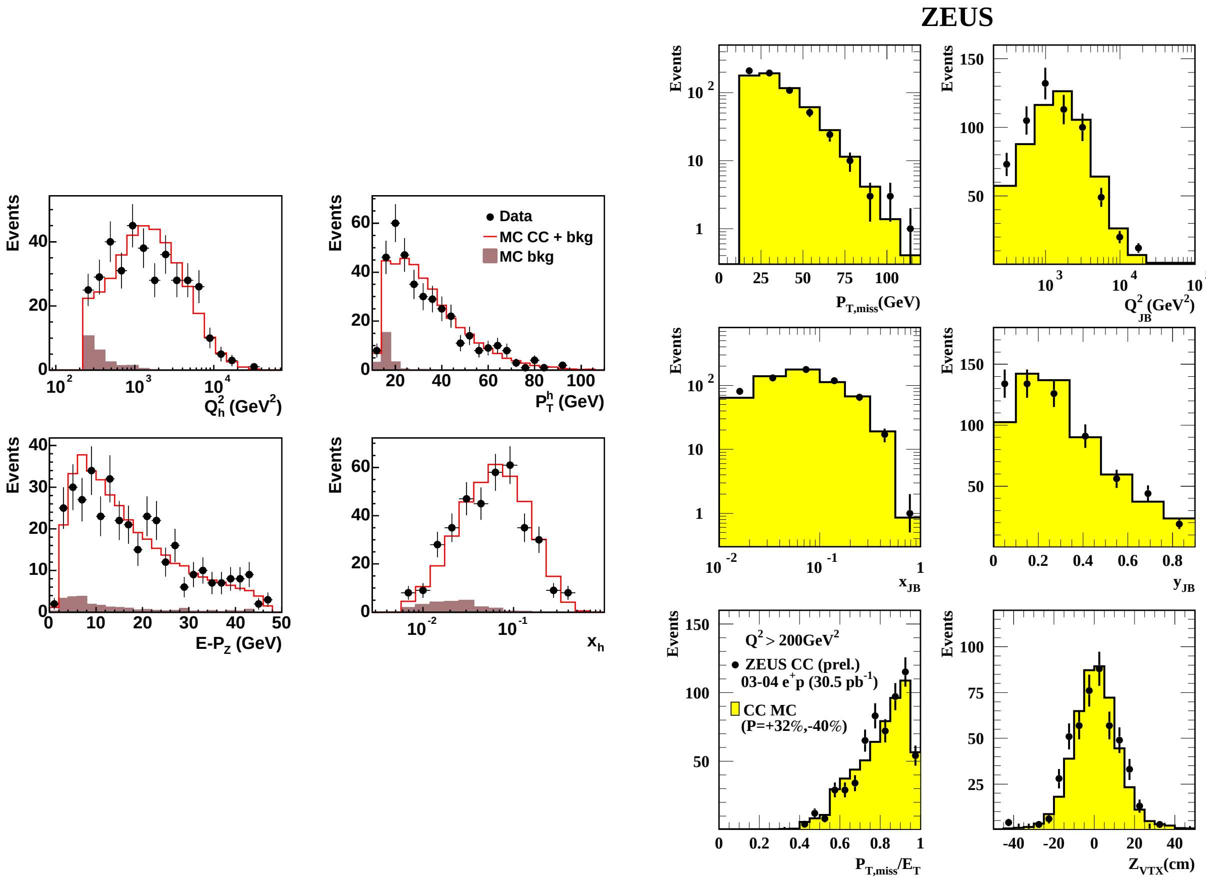

Figure 2: Comparison of the final e^+p CC data samples with the expectation of the Monte Carlo simulation described in the text. On the left the distributions Q^2, $P_{T,\mathrm{miss}}$, $E - P_z$ and x for the right handed H1 CC data sample are shown and on the right $P_{T,\mathrm{miss}}$, Q^2, x, y, $P_{T,\mathrm{miss}}/E_T$ and Z_{VTX} for the ZEUS CC data sample.

5 Event selection

CC events are selected by requiring $P_{T,\mathrm{miss}} > 12\,\mathrm{GeV}$. In order to ensure high trigger efficiency and good kinematic resolution the analysis is restricted to the kinematic region of $Q^2 > 200\,\mathrm{GeV}^2$ and in y by $0.03 < y < 0.85$ for the H1 measurement and $y < 0.9$ for the ZEUS measurement. Non-ep background is rejected by searching for typical beam-induced background event topologies. For the ZEUS measurement a total of 604 candidate events passed the selection criteria. The background contamination was estimated to be typically less than 1% but was as high as 5% in the lowest Q^2 bin of the negative polarisation sample. The contribution of simulated background for the H1 measurement is visible at low Q^2 in Fig. 2. It shows a comparison of data and MC distributions for the CC sample of the H1 and ZEUS measurements. The Monte Carlo gives a good description of the data.

NC events are selected by identifying the scattered electron. For this task sophisticated algorithms are used by both experiments. The main background supression is achieved by requiring a reconstructed scattered electron energy $E'_e > 11\,\mathrm{GeV}$ for H1 and $E'_e > 10\,\mathrm{GeV}$ for ZEUS with additional isolation criteria. The ZEUS analysis selected a total of 52004 candidate events in the kinematic region of $Q^2 > 200\,\mathrm{GeV}^2$ and $y < 0.95$. The background contamination was estimated to be typically less than 1%. Figure 3 shows a comparison of data and MC expectation distributions for the NC sample. The Monte Carlo gives a generally good description of the data. Inaccuracies in the simulation of the scattered positron energy distribution are considered in the corresponding systematic uncertainty. The effects of the positron fiducial-volume cut can be seen in the distribution of the scattered positron angle.

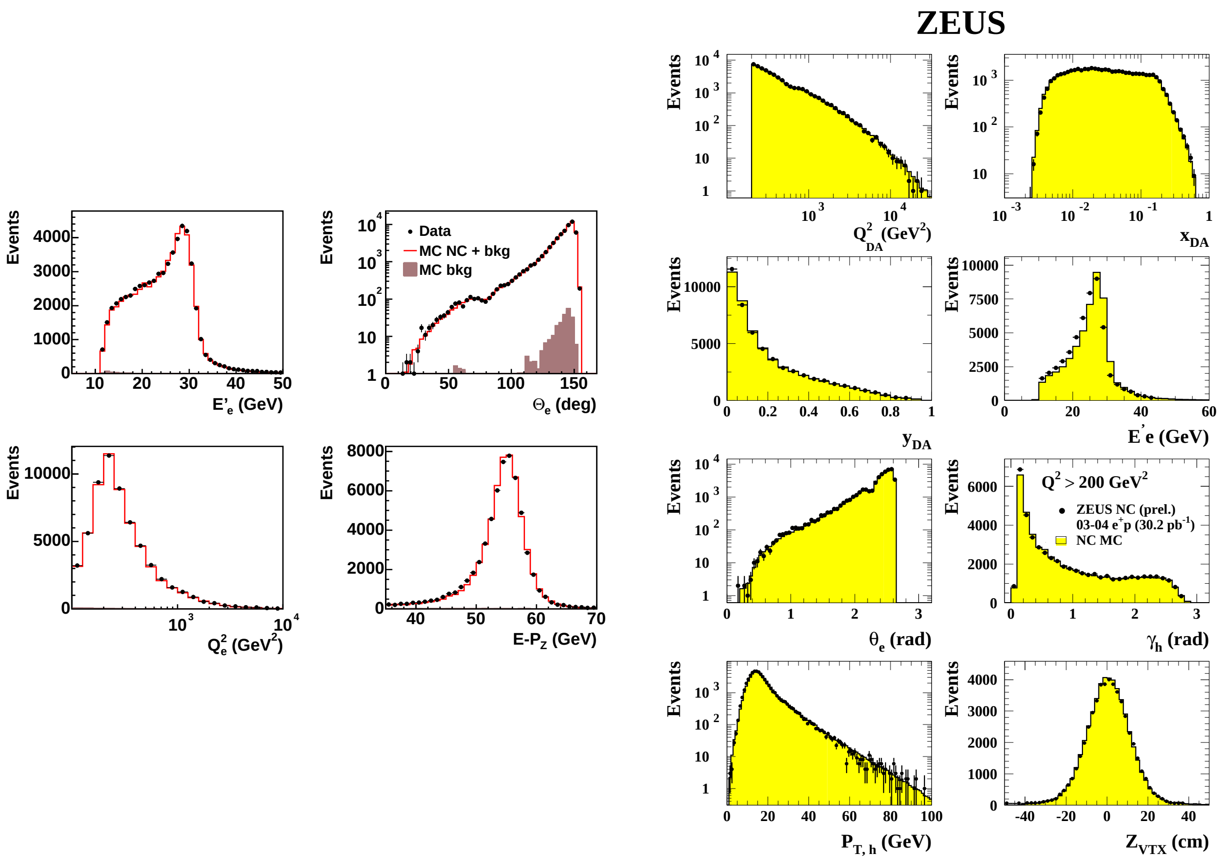

Figure 3: Comparison of the final e^+p NC data samples with the expectation of the Monte Carlo simulation described in the text. On the left the distributions E_e, θ_e, Q^2 and $E - P_z$ for the right handed H1 NC data sample and on the right Q^2, x, y, E'_e, θ_e, γ_h, $P_{t,h}$ and $Z_{\rm VTX}$ for the ZEUS NC data sample are shown.

6 Results

The total cross section for e^+p CC DIS in the kinematic region $Q^2 > 200\,\text{GeV}^2$ was measured by ZEUS at the given longitudinal positron beam polarisations to be:

$$\begin{aligned}\sigma_{\rm CC}(P = 31.8 \pm 0.9\%) &= 46.7 \pm 2.4(\text{stat.}) \pm 1.0(\text{syst.})\text{pb},\\ \sigma_{\rm CC}(P = -40.2 \pm 1.1\%) &= 22.5 \pm 1.6(\text{stat.}) \pm 0.5(\text{syst.})\text{pb}.\end{aligned}$$

Note that the ZEUS measurement does not include the uncertainty in the luminosity of $\pm 5\%$ in the systematic uncertainty. The total cross section is shown as a function of the longitudinal polarisation of the positron beam in Fig. 4 including the unpolarised ZEUS measurement from the 1999-2000 data [2]. The data are compared to the SM prediction evaluated using the ZEUS-S PDFs [16]. The SM prediction describes the data well. The cross section points at polarisations of 31.8% and -40.2% respectively are 3.4 standard deviations above and 6.1 below the unpolarised measurement, respectively.

The single-differential cross-sections, $d\sigma/dQ^2$, $d\sigma/dx$ and $d\sigma/dy$ for charged current DIS are also shown in Fig. 4. A clear difference is observed between the measurements for positive and negative longitudinal polarisation, which is well described over the whole kinematic region by the SM evaluated using the ZEUS-S PDFs.

H1 measured the integrated polarised cross section in the kinematic range $Q^2 > 400\,\text{GeV}^2$ and $y < 0.9$ to be:

$$\begin{aligned}\sigma_{\rm CC}(P = +33 \pm 2\%) &= 34.7 \pm 1.9(\text{stat.}) \pm 1.7(\text{syst.})\,\text{pb},\\ \sigma_{\rm CC}(P = -40.2 \pm 1.5\%) &= 13.8 \pm 1.0(\text{stat.}) \pm 1.0(\text{syst.})\,\text{pb}.\end{aligned}$$

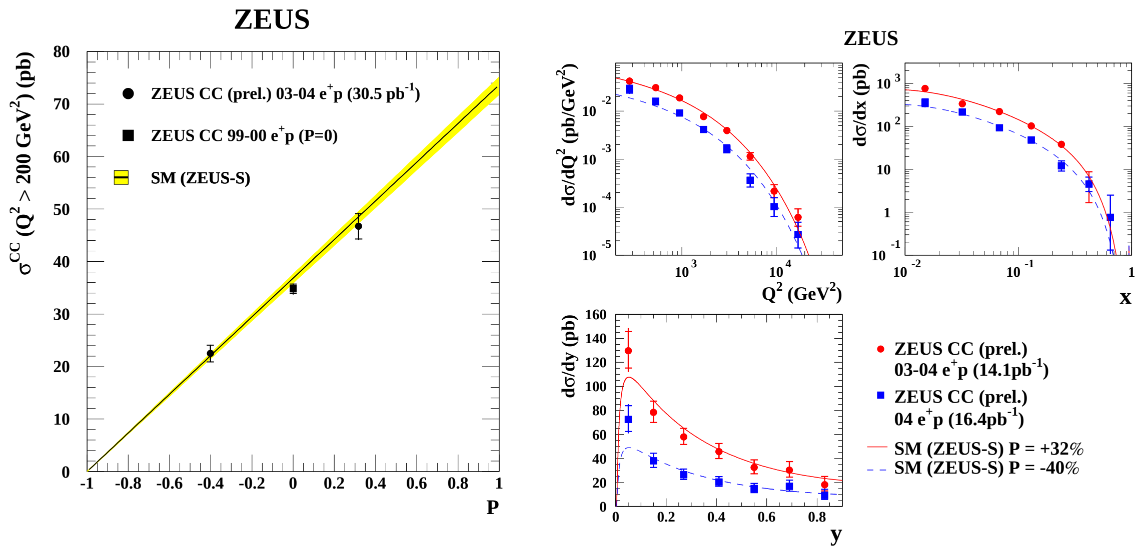

Figure 4: The total cross sections measured by ZEUS are shown on the left against the longitudinal polarisation of the lepton beam. On the right the e^+p DIS CC cross-sections $d\sigma/dQ^2$, $d\sigma/dx$ and $d\sigma/dy$ are shown. The circles (squares) represent the data for positive (negative) polarisation measurements. The curves show the SM prediction evaluated using the ZEUS-S PDFs.

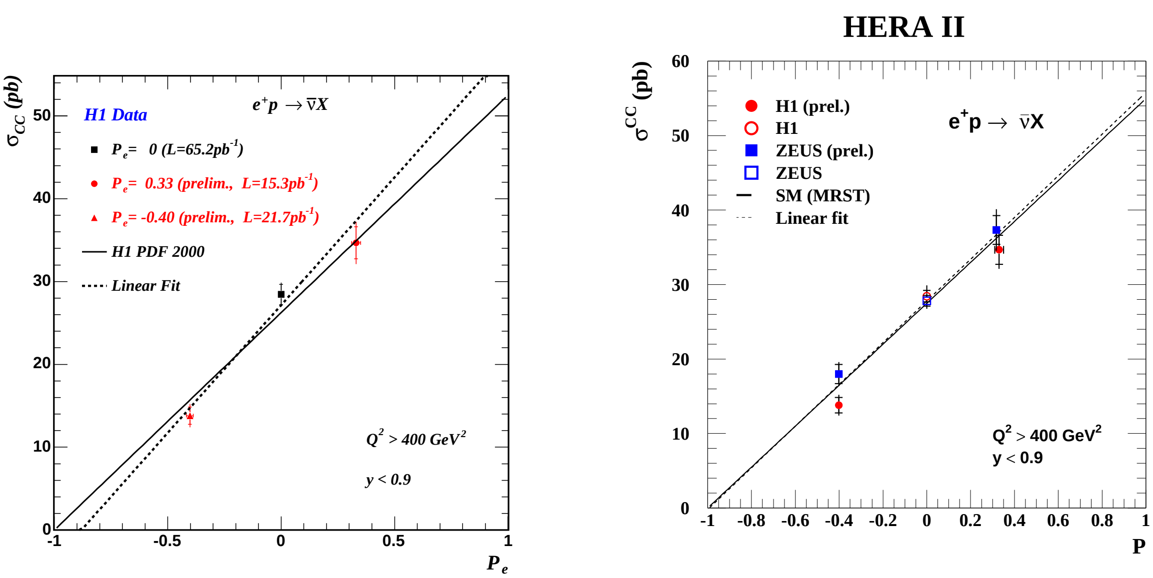

Figure 5: On the left the total e^+p DIS CC cross section measured by H1 is plotted against the longitudinal lepton beam polarisation. The full line shows the SM prediction evaluated using the H1 PDF 2000 fit. The dashed line shows the result of a linear fit to the data. On the right the H1 measurement is compared to the ZEUS result scaled to the same kinematic region.

The total cross section is shown as a function of the longitudinal polarisation together with the unpolarised CC cross section measurement based on the HERA I data set [1] with an integrated luminosity of $65.2\,\text{pb}^{-1}$ in Fig. 5. These are compared to the SM expectation using the H1 PDF 2000 fit [1]. The same figure shows the result of a linear fit to the dependence of the cross section on the longitudinal polarisation describing reasonably the data. Extrapolating the fit to the point $P = -1$ yields:

$$\sigma_{\text{CC}}(P = -1) = -3.7 \pm 2.4(\text{stat.}) \pm 2.7(\text{syst.})\,\text{pb}. \tag{5}$$

This extrapolation is consistent with the SM prediction of zero cross section. The comparison of the H1 results to the ZEUS results scaled to the kinematic region corresponding to the H1 measurement in Fig. 5 shows a good agreement between the two experiments.

The cross-sections $d\sigma/dQ^2$ for NC DIS for positive and negative longitudinal polarisations as measured by ZEUS are shown in Fig. 6 together with the ratios of the cross sections for the positive and negative longitudinal polarisations to the unpolarised results [2]. Also shown is the ratio of the cross sections for the positive and negative longitudinal polarisations. Only statistical uncertainties were considered when taking ratios of the positively and negatively polarised cross sections. In taking ratios to the unpolarised cross sections the systematic uncertainties were considered uncorrelated with those of the polarised cross sections. The measurements are well described by the SM evaluated using the ZEUS-S PDFs and consistent with the expectations of the electroweak SM for polarised NC DIS, although the statistical precision of the current data set does not allow the polarisation effect to be conclusively observed.

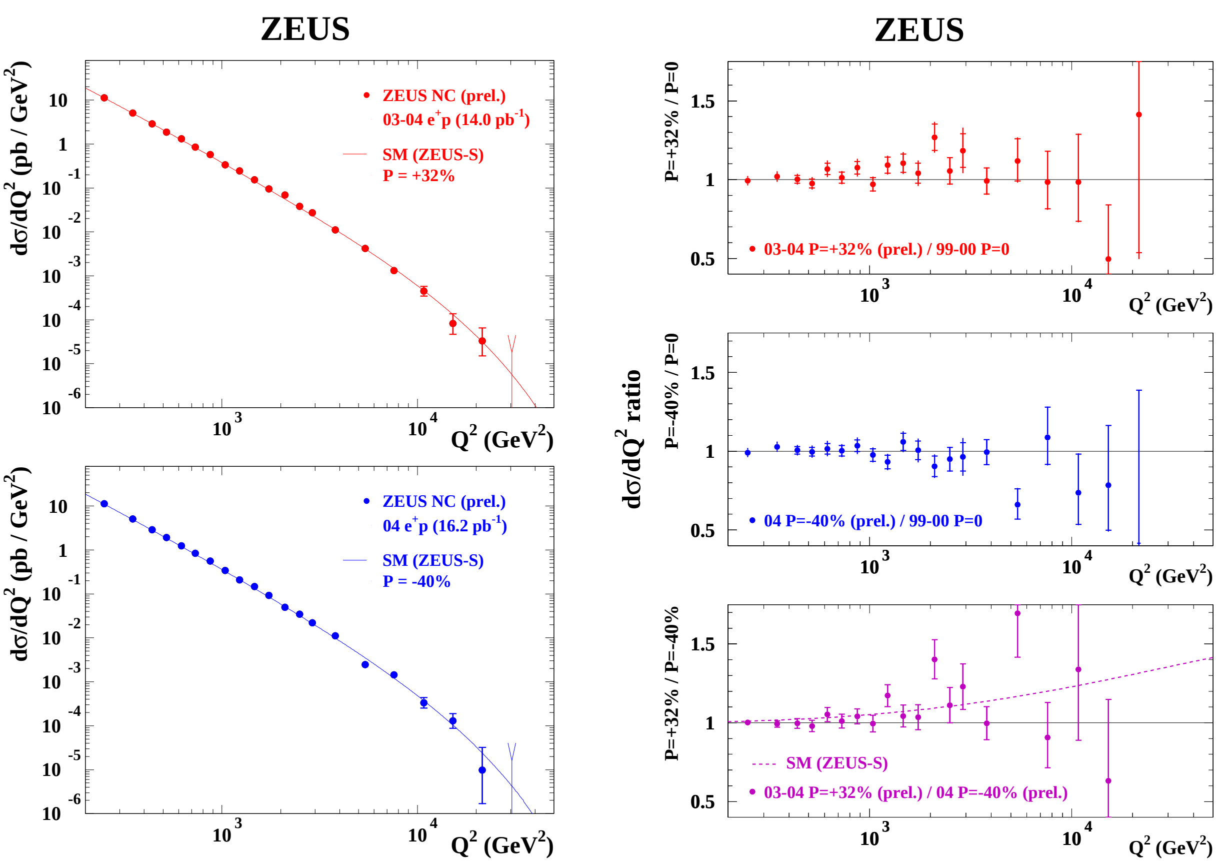

Figure 6: The ZEUS e^+p DIS NC cross-sections $d\sigma/dQ^2$ for positive (upper left) and negative (lower left) polarised data. The curves show the SM prediction evaluated using the ZEUS-S PDFs. On the right the ratios of the NC DIS cross sections $d\sigma/dQ^2$ for the positively polarised data to unpolarised data (upper), negatively polarised data to unpolarised data (middle) and positively polarised data to negatively polarised data are shown. The dashed curve shows the SM prediction evaluated using the ZEUS-S PDFs.

References

1. H1 Coll., C. Adloff et al.., Eur. Phys. J. C **30** (2003) 1, and references therein.
2. ZEUS Coll., S. Chekanov et al., Eur. Phys. J. C **32**, 1 (2003);
   ZEUS Coll., S. Chekanov et al., Phys. Rev. D **70** (2004) 052001, and references therein.
3. CDHS Coll., H. Abramowicz et al., Z. Phys. **C 25**, 29 (1984);
   CDHSW Coll., J.P. Berge et al., Z. Phys. **C 49**, 187 (1991);
   CCFR Coll., E. Oltman et al., Z. Phys. **C 53**, 51 (1992);
   BEBC Coll., G.T. Jones et al., Z. Phys. **C 62**, 575 (1994).
4. A. A. Sokolov and I. M. Ternov, Phys. Dokl. **8** (1964) 1203.
5. D. P. Barber *et al.*, Nucl. Instrum. Meth. A **329**, 79 (1993).
6. M. Beckmann *et al.*, Nucl. Instrum. Meth. A **479** (2002) 334.
7. R.J. Cashmore et al., *Proc. the Workshop on Future Physics at HERA*, G. Ingelman, A. De Roeck and R. Klanner (eds.), Vol. 1, p. 163. DESY, Hamburg, Germany (1996)
8. F. Jacquet and A. Blondel, *Proceedings of the Study for an ep Facility for Europe*, U. Amaldi (ed.), p. 391. Hamburg, Germany (1979). Also in preprint DESY 79/48
9. S. Bentvelsen, J. Engelen and P. Kooijman, *Proc. Workshop on Physics at HERA*, W. Buchmüller and G. Ingelman (eds.), Vol. 1, p. 23. Hamburg, Germany, DESY (1992);
   K.C. Höger, *Proc. Workshop on Physics at HERA*, W. Buchmüller and G. Ingelman (eds.), Vol. 1, p. 43. Hamburg, Germany, DESY (1992).
10. U. Bassler and G. Bernardi, Nucl. Instrum. Meth. A **361**, 197 (1995);
    U. Bassler and G. Bernardi, Nucl. Instrum. Meth. A **426**, 583 (1999).
11. G.A. Schuler and H. Spiesberger, *Proc. Workshop on Physics at HERA*, W. Buchmüller and G. Ingelman (eds.), Vol. 3, p. 1419. Hamburg, Germany, DESY (1991);
    H. Spiesberger, HERACLES *and* DJANGOH*: Event Generation for ep Interactions at HERA Including Radiative Processes*, 1998, available on `http://www.desy.de/ hspiesb/djangoh.html`.
12. L. Lönnblad, Comp. Phys. Comm. **71**, 15 (1992).
13. T. Sjöstrand, Comp. Phys. Comm. **39**, 347 (1986);
    T. Sjöstrand and M. Bengtsson, Comp. Phys. Comm. **43**, 367 (1987);
    T. Sjöstrand, Comp. Phys. Comm. **82**, 74 (1994).
14. G. Marchesini et al., Comp. Phys. Comm. **67**, 465 (1992).
15. H. Jung, Comp. Phys. Comm. **86**, 147 (1995).
16. ZEUS Coll., S. Chekanov et al., Phys. Rev. **D 67**, 012007 (2003).